2010

A study on saline water intrusion and fresh water recharge relevant to coastal environment

Sudip Basack
Bengal Engineering and Science University, sudip@uow.edu.au

Amartya Kumar Bhattacharya
Bengal Engineering and Science University

Chitta Sahana
Bengal Engineering and Science University

Prabir Maity
Bengal Engineering and Science University

Publication Details

Basack, S., Bhattacharya, A. K., Sahana, C. & Maity, P. (2010). A study on saline water intrusion and fresh water recharge relevant to coastal environment. WSEAS Transactions on Fluid Mechanics, 5 (3), 80-90.

A study on saline water intrusion and fresh water recharge relevant to coastal environment

Abstract
The paper is based on experimental laboratory model study with relevant mathematical analysis followed by field investigation so as to understand the characteristics and flow pattern of saline water intrusion into natural porous medium followed by subsequent fresh water recharge.

Keywords
recharge, environment, fresh, coastal, intrusion, water, saline, study, relevant

Publication Details
Basack, S., Bhattacharya, A. K., Sahana, C. & Maity, P. (2010). A study on saline water intrusion and fresh water recharge relevant to coastal environment. WSEAS Transactions on Fluid Mechanics, 5 (3), 80-90.

A Study on Saline Water Intrusion and Fresh Water Recharge relevant to Coastal Environment

SUDIP BASACK A K BHATTACHARYA CHITTA SAHANA PRABIR MAITY
Department of Applied Mechanics
Bengal Engineering and Science University
Shibpur, Howrah 711103
INDIA
basackdrs@hotmail.com http://www.becs.ac.in/appliedmechanics_sbasak.html

Abstract: - The paper is based on experimental laboratory model study with relevant mathematical analysis followed by field investigation so as to understand the characteristics and flow pattern of saline water intrusion into natural porous medium followed by subsequent fresh water recharge.

Key-Words: - Coastal aquifer, Darcy flow, Forchheimer flow, Fresh water recharge, Reynolds number, Saline water intrusion.

1 Introduction

The seepage of saline water from sea into the adjacent coastal aquifers is particularly called saline water intrusion (SWI). Similarly, the discharge of fresh water seeping into the aquifer from nearby fresh water aquifers or a surface water source is specifically called fresh water recharge.

A review of literature indicates significant contribution in related areas. The works of Cooper (1964), Dagan & Bear (1968), Taniguchi *et al.* (2001), and Bhattacharya *et al.* (2004) are worthy of note. Some of these works are analytical while the others have been laboratory and field investigations.

Previous investigations in this field were based on an assumption mixing between fresh water and saline water occurs as a sharp interface. But this assumption deviates from reality to a great extent since quite naturally there always exists a brackish transition zone where diffusion between fresh water and saline water takes place. This needs a detailed investigation. The work reported herein is aimed towards conducting a thorough laboratory model study subsequently followed by theoretical analysis involving study on saline water intrusion into natural porous media (fine sand bed) and subsequent fresh water recharge.

2 Theoretical Considerations

2.1 Type of Porous Media

Most materials are porous when viewed at an appropriate length scale. Examples range from porous silicon, which is porous on the nanometre scale to limestone caves and underground river system on the kilometre scale. However of this work it can be placed under two categories.

Category-1: This category includes those porous media which has no individual particle but consist of a definite matrix. The shape of the matrix is distorted under the fluid flow conditions. The best example of this category is sponge.

Category-2: This category includes porous media such as sand or glass beads packed in a fixed volume. In this type of porous media individual particles get distorted from their original position during the flow of fluid. Sand and glass beads may be differ in their properties, i.e., surface roughness and size of the particles. Surface and size of the glass beads are smoother and more uniform as compared to the sand particles.

Flow of fluid through a porous medium is basically governed by its porosity and the hydraulic conductivity.

2.2 Properties of Flow through Porous Media

The properties which govern the flow through a porous media are sequentially described below:

1. Porosity: porosity is a dimensionless quantity denoted by φ. It is the ratio of void space to the total volume of material. It dictates how much fluid a saturated material can contain and has an important influence on bulking properties of the material.

2. Permeability: Permeability is a measure of the ability of a material to transmit fluid under a hydraulic gradient. Permeability is a function of porous media only.

3. Hydraulic conductivity: It may be defined as the fluid velocity per unit hydraulic gradient. It is a function of both the porous medium and fluid. It is denoted as K and in mathematical expression

$$K = -\frac{V}{\left(\frac{dh}{dx}\right)}$$

Where, $\frac{dh}{dx}$ = hydraulic gradient.

K= hydraulic conductivity.

V= mean velocity of flow or volume rate of flow / unit area.

Hydraulic conductivity has the same unit as that of velocity i.e., (m/s).

Owing the failure at the present time to attain more than a moderately valid expression relating the coefficient of permeability to the geometric characteristics of soil, refinement in K are hardly warranted. However, because of the influence that the density and viscosity of the pore fluid may exert on the resulting velocity, it is some value to isolate that part of K which is dependent on these properties. To do this, the term physical permeability K_0 (square centimetres) was introduced, which is a constant typifying the structural characteristics of the medium and is independent of the property of the fluid. The relationship between the permeability and the coefficient of permeability as given by Muskat (1995) is,

$$K = k_0 \frac{\gamma_w}{\mu}$$

Where, γ_w is the unit weight of the fluid and μ is the coefficient of viscosity. Substituting in equation (a) in to Darcy's law,

$$K = k_0 \frac{\gamma_w}{\mu} \frac{dh}{dx}$$

This indicates that the discharge velocity is inversely proportional to the viscosity of the fluid. Some typical values of the coefficient of permeability of different natural porous media are presented in Table-1.

Table 1. Some Typical Values of Coefficient of Permeability

Soil Type	Coefficient of permeability k, cm/sec
Clean grave	1.0 and greater
Clean sand (coarse)	1.0 - 0.01
Sand (mixture)	0.01 - 0.005
Fine sand	0.05 - 0.001
Silt	0.0005 - 0.00001
Clay	0.000001 and smaller

The coefficient of permeability is another function of both soil and fluid property. If,

$$q_i = -k \frac{\partial h}{\partial x_i} \quad (i=1,2,3)$$

Then this k depends on the properties of both solid and fluid aspects of porous media and is given by,

$$K = \frac{k \rho g}{\mu}$$

Where, g is the gravitational acceleration, μ is viscosity of pore fluid and k is the permeability having the dimension of (length)^2 . This k is independent of the properties of fluid and will depend only on the porosity.

2.3 Types of Flow Through Porous Media

Depending upon the Reynolds Number, flow through porous media can be broadly categorized as *Laminar* flow and *Turbulent* flow.

2.3.1 Laminar Flow

There are many instances of flow of fluid through porous media. For example, the movement of water, oil, and natural gas through the ground, seepage underneath dams and large buildings, flow through packed towers in some chemical process, filtration, all this depend on this flow.

The velocity of these cases is usually so small and flow passages so narrow that laminar flow may be assumed without hesitation. The laminar flow through porous media can be either linear or non-

linear as investigated by many in their separately conducted experiments. However the results of Darcy and Forchheimer are most challenging.

(a) Linear Flow

Linear flow regimes consist of Darcy and pre-Darcy flow. However as the sensitivity of available instrumentation is not sufficient to measure the extremely low pressure gradient and velocities, only Darcy flow is analyzed.

In 1856, the French engineer Henri Darcy performed experiments on the flow of water through a pipe packed with sand and discovered that certain conditions the volume rate of flow through the pipe was proportional to the negative of the pressure gradient. This relationship which is called Darcy's law, can be stated as follows :

$$V = -K\frac{dh}{dx}$$

Where, $\frac{dh}{dx}$ = hydraulic gradient

K = hydraulic conductivity

V = mean velocity of flow or volume rate of flow per unit area

The negative sign in the equation indicates that the flow is always in the direction of decreasing head. Subsequent research has modified the Darcy law to include the fluid viscosity and can be stated as

$$V = -\frac{K}{\mu}\frac{dp}{dx}$$

Where, μ = dynamic viscosity of pore fluid.

The value of K in the equation depends not only on the viscosity of fluid but also on the size and geometrical arrangement of the solid partials in the in the porous material. It is thus difficult to predict the value of K appropriate to the particular set of conditions. As the Darcy's law expresses a linear equation, the flow governed by this law definitely is a linear flow. The Reynolds number corresponding to the lower and upper bound of Darcy regime can be designated by R_{eDL} and R_{eDH} respectively.

Visual observation of dyes injected into liquids led Reynolds in 1883, to conclude that the orderliness of the flow was dependent on its velocity. At small velocities the flow appeared orderly, in layers, that is, laminar. With increasing velocities, Reynolds observed a mixing between the dye and water; the pattern of flow becomes irregular, or turbulent.

Within the range of laminar flow, Reynolds found a linear proportionality to exist between hydraulic gradient and velocity of flow, in keeping the Darcy's law. With the advent of turbulence, the hydraulic gradient approached the square of the velocity. These observations suggest a representation of the hydraulic gradient as :

$$i = av + bv^n$$

Where, 'a' and 'b' are consists and 'n' is a real quantity between 1 and 2. There remains now the equation of the determination of the laminar range of the flow and the extend to which actual flow systems through soils are included. Such a criterion is furnished by Reynolds number R_e (a pure number related inertial to viscous force), defined as,

$$R_e = \frac{\rho V d}{\mu}$$

Where, V = superficial flow velocity,
d = Mean sand diameter,
ρ = Density of fluid,
μ = Dynamic viscosity of fluid,

Particle Reynolds number for Darcy flow 1.5×10^{-5} to 2.3×10^{-5}.

(b) Non-Linear or Forchheimer Flow

Linear or Darcy flow is an expression of dominance of viscous forces applied by the solid porous matrix on the interstitial fluid and is of limited applicability. But non-Darcy or post Darcy flow is affected by inertia forces and turbulence. Forchheimer is widely regarded as being the first to suggest a non-linear relationship between the pressure gradient and fluid velocity for $R_e > R_{eDH}$. Generalizing Forchheimer's equation is given as,

$$-\frac{dh}{dx} = \frac{1}{\gamma}\left(aV + bV^2\right)$$

Where, $\frac{dh}{dx}$ = hydraulic gradient

γ = specific weight

V = volume rate of flow per unit area

And 'a' and 'b' are coefficients.

Particle Reynolds number for Darcy flow ranges between 1.5×10^{-5} to 2.3×10^{-5}.

Particle Reynolds number for Forchheimer flow ranges between 2.3×10^{-5} to 80 x 10^{-5}.

2.3.2 Turbulent Flow

The term turbulent or Post Forchheimer Flow refers to flow for which $R_e > R_{eFH}$, that is, for Reynolds number higher than those for which Forchheimer flow occurs. There is a translation from laminar to turbulent flow to be the particle Reynolds Number (R_{eFH}).

3 Laboratory Experimentation

3.1. Experimental Set Up

In order to carry out model tests so as to study the pattern of seepage in regards to saline water intrusion and freshwater recharge into natural porous medium, an experimental set up has been developed. A sketch of this apparatus is shown in Fig.1. A photographic view of this test set up is presented in Fig.2.

The entire set up has been fabricated with 5 mm thick transparent Perspex sheet. It is mainly consists of inlet tank, a rectangular open channel, a gate and out let tank. In the middle of the open channel, a sliding gate is provided which is capable to a unidirectional up-down movement which is governed by a rope and pulley arrangement. The function of this gate is to provide variable opening of the flow passage. The hydraulic connections between the two tanks with the channel is done by cast iron pipes with inlet and outlet valves. One of the side walls of the central channel is graduated with square grid so as to trace the phreatic line of salt water and also the interface between saline water and fresh water. The side walls of the two tanks are also graduated so as to measure the inlet and outlet heads. The entire set up is fixed on a wooden table.

3.2. Test Procedure

Initially, the central channel is filled with the porous medium upto the desired level. The gate level is adjusted as per requirement. The gate is to be inserted within the porous medium with extreme such that the porosity of the medium gets disturbed to a minimum. In one of the two tanks, salt water having a specified saline concentration is poured upto the desired head. For visualization purpose, this salt water should be preferably coloured by an inert material. The valve between this tank and the channel is opened and a stopwatch is started. It should be ensured that the valve between the other tank and the channel is fully closed. After regular interval, the pattern of intrusion is noted from the coordinates phreatic line corresponding to the seepage of saline water. After hydraulic stabilization is achieved, the heads at the upstream and the downstream ends as well as the coordinates of the stabilized phreatic line are noted. The other tank is then filled up with fresh water upto desired head and the valve is opened. The continuous flow of water in this inlet tank should be ensured. At regular intervals, the shifting of the locations of the surface of salt water is noted.

3.3 Determination of Forchheimer's Coefficients

The Forchheimer's coefficients 'a' and 'b' for different pore fluids can be determined using the test set up. Before finding out these coefficients, the Reynolds number has to be checked. Operating the gate of the channel, an additional reading has to be taken so as to ensure that the Reynolds number is in the range of Forchheimer's flow. Then, making the gate opening in the near range, few readings should be taken in regards to the heads at upstream and downstream ends. Calculating the flow velocities, the average values of the Forchheimer's coefficients may be estimated.

4 Porous Media And Saline Water

4.1 Porous Media Used

Uniformly graded fine grained yellow sand having particle sized ranging between 600 μm to 75 μm. The engineering properties of the sand is described in the following sections. The central channel is filled up with this sand by means of rainfall technique from a uniform height of 1 m.

4.1.1 Particle Size Distribution

Dry yellow sand available from local market is sieved between 600 μm to 75 μm to obtained the desired fine grained natural porous medium. The result of sieve analysis of the material is shown in Fig.3. The uniformity coefficient was found to be 6, indicating uniform to medium graded soil.

4.1.2 Various Geotechnical Properties

The geotechnical properties of the sand used in experimentation is shown in Table-2.

Table-2 : Geotechnical properties of the sand used

Sl. No.	Properties	Values
1	Specific gravity of particles (G)	2.655
2	Unit weight of the prepared sand bed (γ)	14.7 KN/m^2
3	Relative Density of the prepared sand bed (D_r)	70.4 %

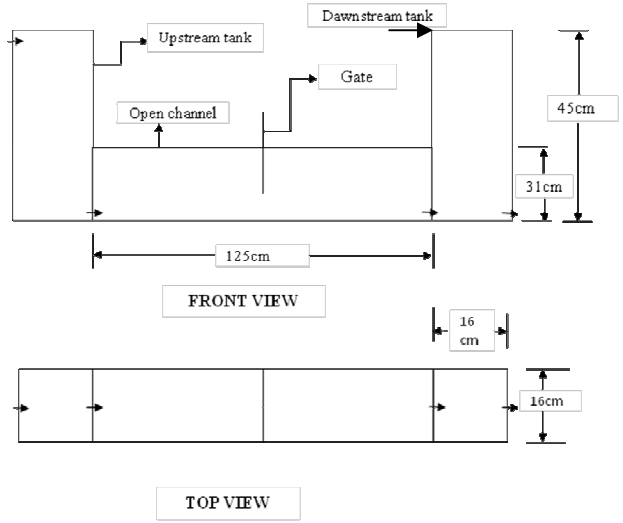

Fig.1. Schematic diagram of the experimental set up.

Fig.2. Photographic views of test set up.

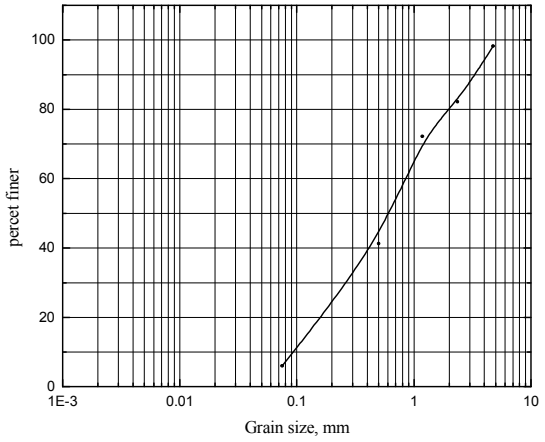

Fig. 3. Grain Size Distribution curve.

4.2 Saline Water

Pure Sodium Chloride is dissolved into distilled water at a specified concentration so as to obtain the saline water. A small quantity of $KMnO_4$ is used as the colouring dye such that its presence does not significantly affect the density and other hydraulic property of the solution. The different properties of the saline water have been described below.

4.2.1 Kinematic Viscosity at different Temperatures

The maximum solubility of the sodium chloride in distilled water at room temperature (30^0C) was determined as 35.7×10^4 mg/L. This saturated solution was used during actual experimentation. However, the kinematic viscosity of the solution at different temperatures and different saline concentrations are determined in the laboratory with the help of Saybolt's Universal Viscometer. The values are presented in Table-3.

Table-3 : Kinematic Viscosity of Saline Water

Salinity Concentration (mg/L)	Temperature (^{0}c)	Kinematic Viscosity ($10^{-7}m^2$/sec)
35.7×10^4	20	18.51
	25	18.47
	26	18.41
	30	18.33
	32	18.26
	40	17.58
31.3×10^4	20	15.1
	25	15.0
	26	14.98
	30	14.94
	32	14.87
	40	13.38
0	20	10.21
	25	10.13
	26	10.1
	30	10.06
	32	10.0
	40	10.44

4.2.2 Hydraulic Conductivity

The Darcy's coefficient is determined using a falling head permeameter with the sand media at the particular density and concentrated saline water as the pore fluid. The value was determined as 0.5936×10^{-4} cm/sec. The Forchheimer's coefficients, as determined using the test set up

itself, came out to be : a = 0.1168×10^{-2}, and b = 0.6327×10^{-5}.

4.3. Fresh Water

During experimentations, distilled water has been used as the fresh water. Since all the hydraulic characteristics of the same are standardised, these are not determined separately.

5 Mathematical Analysis

5.1. Suggested Values of 'a' and 'b' and Relation between them

The suggested values of 'a' and 'b' as per Ergun (1952), are : Range of a = 150 to 180 ; Range of b= 1.75 to 1.8. The relation between these two parameters may be obtained from the graph shown in Fig.4.

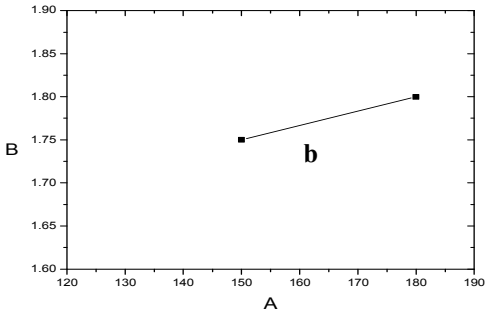

Fig.4. Graph showing relation between a & b.

From the graph, it may be noted that the relation between 'a' and 'b' is linear and may be expressed as,

$$b=0.0017a+1.5$$

5.2. Recasting of Forchheir's Law making Velocity as the Subject of Formulae

The non-linear Forchheimer's equation is rewritten making velocity as independent variable.

$$-\frac{dh}{dx}=\frac{1}{\gamma}(aV+bV^2) \qquad ...(1)$$

This may be re-written as,

$$V=-\frac{a}{2b}\left(1\pm\sqrt{1+\frac{4b\gamma i}{a^2}}\right) \qquad ...(2)$$

Expanding $\left(\sqrt{1+\frac{4b\gamma i}{a^2}}\right)$ by binomial expansion, the following equation is obtained:

$$\sqrt{\left(1+\frac{4b\gamma i}{a^2}\right)}=1+\frac{1}{2}\left(\frac{4b\gamma i}{a^2}\right)-\frac{1}{8}\left(\frac{4b\gamma i}{a^2}\right)^2+\frac{1}{16}\left(\frac{4b\gamma i}{a^2}\right)^3-\frac{5}{128}\left(\frac{4b\gamma i}{a^2}\right)^4$$

Truncating the right hand side of the above equation after the 5th term and substituting, the expression for velocity becomes

$$V=\frac{a}{2b}\left[\frac{1}{2}\left(\frac{4b\gamma i}{a^2}\right)-\frac{1}{8}\left(\frac{4b\gamma i}{a^2}\right)^2+\frac{1}{16}\left(\frac{4b\gamma i}{a^2}\right)-\frac{5}{128}\left(\frac{4b\gamma i}{a^2}\right)^4\right]$$

...(3)

The reason for taking negative sign is obvious because at is i=0, V=0

It is usually sufficient for a non-linear analysis to consider up to the quadratic term only and in that case V becomes,

$$V=\frac{a}{2b}\left[\frac{1}{2}\left(\frac{4b\gamma i}{a^2}\right)-\frac{1}{8}\left(\frac{4b\gamma i}{a^2}\right)^2\right]$$

That is, $V=\frac{\gamma i}{a}-\frac{b\gamma^2 i^2}{a^3}$ ...(4)

5.3. Expansion of Forchheimer's Equation in Terms of 'a' and 'b'

Using the earlier analysis of Bhattacharya et al. (2004), the above equation can be expressed as,

$$V=\frac{\gamma i}{a}-\frac{b}{a^3}(\gamma i)^2$$

$$V=\frac{\gamma i\phi^3 d^2}{A(1-\phi)^2\mu}(i)-\frac{B}{A^3}\frac{\phi^6\rho d^5\gamma^2}{(1-\phi)^5\mu}(i)^2 \qquad ...(5)$$

Substituting Ergun's 'b' in terms of 'a',

$$V=\left\{\frac{\phi^3 d^2 g}{A(1-\phi)^2\nu}\right\}(i)-\left\{\frac{(0.0017A+1.5)}{A^3}\frac{\phi^3 d^5 g^2}{(1-\phi)^5\nu}\right\}(i)^2$$

...(6)

5.4. Expansion of Forchheimer's Law in terms of Modified Reynolds Number and Friction Factor

Re-writing the above equation,

$$-\frac{dp}{dx} = A\frac{(1-\phi)^2}{\phi^3}\frac{\mu V}{d^2} + B\frac{(1-\phi)}{\phi^3}\frac{\rho V^2}{d} \quad ...(7)$$

Dividing both sides by $B\frac{(1-\phi)}{\phi^3}\frac{\rho V^2}{d}$, the equation becomes,

$$-\frac{dp}{dx}\frac{d\phi^3}{BV^2(1-\phi)\rho} = \frac{A(1-\phi)\mu}{Bd\rho V} + 1 \quad ...(8)$$

The left hand side of the equation (3.18) can be compared with **Darcy Weisbach's friction factor** C_f **.**

Darcy Weisbach's friction factor $C_f = \frac{\nabla p}{L}\frac{D}{\nu V^2}\frac{2g}{\rho}$

$$= \frac{\nabla p}{L}\frac{D}{\nu V^2}\frac{numericalvalue}{\rho} \quad ...(9)$$

Hence the term $-\frac{dp}{dx}\frac{d\phi^3}{BV^2(1-\phi)\rho}$ can be written as a form of friction factor and can be called **Modified Friction Factor** C_f'. So, the term can be expressed as,

$$C_f' = -\frac{dp}{dx}\frac{\phi^3 d}{BV^2\rho(1-\phi)} \quad ...(10)$$

Similarly, the term $\frac{B}{(1-\phi)}\frac{\rho V d}{\mu}$ can be written as **Modified Reynolds Number** (R_e') as compared to actual Reynolds number i.e., $R_e = \frac{\rho V d}{\mu}$

Therefore, $R_e' = \frac{B}{(1-\phi)}\frac{\rho V d}{\mu}$ ...(11)

Thus Modified Friction Factor **(** C_f' **)**

$$C_f' = \frac{1}{R_e'} + 1 \quad ...(12)$$

6 Results And Discussions

6.1 Model Tests

Two different sets of experiments, one for saline water intrusion and another for fresh water recharge were conducted. The heads applied were 20 cm and 30 cm respectively. The test results are presented in Tables 4 & 5 and Figs. 5 & 6 respectively. The x-coordinates are normalized by the distance between inlet and outlet points of the channel. The y-coordinates, on the other hand, are normalized by the head applied in saline water intrusion.

The phreatic lines in saline water intrusion and the interfaces in fresh water recharge are observed to be irregular in pattern as per Figs. 5 & 6. In case of saline water intrusion, the phreatic line at any time instance slopes down from the inlet end with a sudden change in slope at a normalized distance of 0.3 to 0.5. With the advent of time, the phreatic line translates gradually towards the other end of the channel. For fresh water recharge, the interface gradually slopes towards the downstream end in advent of time. The time variation of normalized y-coordinates of the interface at different locations is shown in Fig.7. Although the pattern of variation is irregular in this case, the slopes are observed to be sufficiently small. More importantly, diffusion between fluids of two different densities is observed to take place indicating absence of any sharp interface at mixing zone.

6.2 Mathematical Analysis

The relation between friction factor and Reynolds number for Darcy and Forchheimer flow obtained from mathematical analysis, is shown in Fig.8. The graphical representation of modified Reynolds number versus modified friction factor for different salinity is depicted in Fig.9.

7 Field Investigation

The district of Purba Medinipur is situated on the east coast of West Bengal, India. The aquifers of the districts are contaminated by saline water intrusion. To study the extent and degree of salt water contamination in the coastal zones, water samples were collected from tube wells at 28 various locations of the district [Fig.10]. Chemical Analysis of the water samples so collected were carried out. The relevant results are presented in Table-6 below. From the results, the probable path of saline water ingress is estimated, as shown in Fig.11. The contours of chloride content and total dissolved solids are shown in Figs. 12 & 13 respectively.

Table-4: Normalised coordinates of phreatic line for saline water intrusion

Point No.	X-coordinate value	Y-coordinate value at different time (t in hours)						
		t=2	t=6	t=14	t=16	t=19	t=22	t=34
1	0.0083	0.5	0.613	0.75	0.75	0.75	0.772	0.863
2	0.0416	0.45	0.59	0.727	0.77	0.77	0.818	0.909
3	0.08	0.409	0.545	0.659	0.77	0.77	0.84	0.932
4	0.125	0.386	0.486	0.613	0.704	0.727	0.795	0.795
5	0.166	0.34	0.441	0.568	0.659	0.65	0.727	0.75
6	0.208	0.26	0.363	0.523	0.609	0.636	0.682	0.704
7	0.25	0.136	0.318	0.386	0.545	0.591	0.613	0.613
8	0.291	0.136	0.272	0.341	0.386	0.545	0.568	0.568
9	0.333	0.113	0.163	0.25	0.295	0.309	0.477	0.523
10	0.375		0.127	0.204	0.25	0.272	0.341	0.341
11	0.416		0.136	0.136	0.204	0.227	0.272	0.316
12	0.458		0.113	0.113	0.182	0.204	0.272	0.318
13	0.5		0.9	0.113	0.182	0.204	0.272	0.295
14	0.542				0.182	0.204	0.275	0.275
15	0.583				0.204	0.204	0.227	0.295
16	0.625				0.182	0.182	0.222	0.272
17	0.666				0.172	0.172	0.204	0.25
18	0.708				0.113	0.113	0.182	0.204
19	0.75					0.113	0.136	0.182
20	0.791						0.113	0.136
21	0.875							0.118
22	0.916							0.113

Table-5: Normalised coordinates of phreatic line for fresh water recharge

Point No.	X-coordinate value	Y-coordinate value at various time (t in hours)						
		t=2	t=6	t=14	t=16	t=19	t=22	t=34
1	0.0083	0	0	0	0	0	0	0
2	0.0416	0	0	0	0	0	0	0
3	0.08	0.09	0	0	0	0	0	0
4	0.125	0.136	0.09	0	0	0	0	0
5	0.166	0.191	0.113	0.09	0	0	0	0
6	0.208	0.222	0.136	0.113	0.09	0	0	0
7	0.25	0.258	0.204	0.136	0.113	0.09	0	0
8	0.291	0.277	0.227	0.204	0.136	0.09	0	0
9	0.333	0.295	0.277	0.227	0.227	0.136	0.09	0
10	0.375	0.295	0.277	0.277	0.285	0.227	0.113	0
11	0.416	0.295	0.285	0.285	0.295	0.354	0.285	0.09
12	0.458	0.328	0.295	0.295	0.354	0.398	0.295	0.136
13	0.5	0.328	0.328	0.328	0.398	0.558	0.398	0.285
14	0.542	0.341	0.354	0.354	0.558	0.586	0.558	0.586
15	0.583	0.386	0.398	0.398	0.586	0.698	0.586	0.698
16	0.625	0.568	0.586	0.586	0.698	0.772	0.698	0.772
17	0.666	0.615	0.698	0.698	0.772	0.818	0.84	0.84
18	0.708	0.704	0.772	0.772	0.818	0.84	0.84	0.909
19	0.75	0.727	0.818	0.818	0.84	0.909	0.909	0.932
20	0.791	0.75	0.84	0.84	0.909	0.909	0.932	1
21	0.875	0.772	0.909	0.909	0.909	0.932	1	1
22	0.916	0.909	0.909	0.909	0.932	1	1	1
23	0.958	0.909	0.932	0.932	1	1	1	1
24	1	0.909	1	1	1	1	1	1

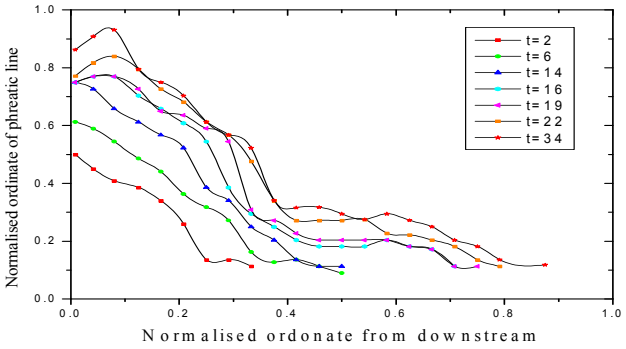

Fig.5. Graphical representation of the experimental results for Saline water intrusion.

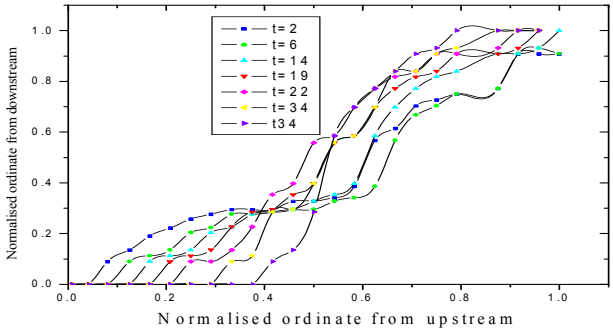

Fig.6. Graphical representation of the experimental results for fresh water recharge.

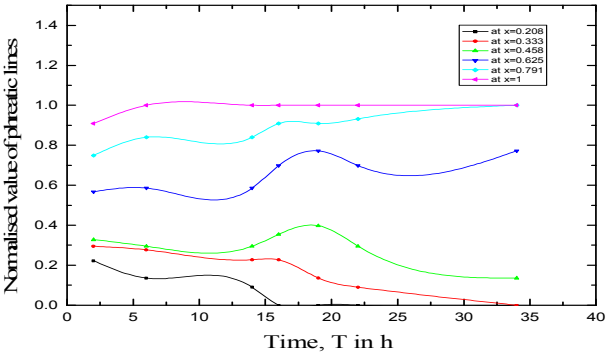

Fig.7. Graphical representation of the stratified fluid (in constant ordinate values from upstream) in various times vs. normalised value of abscissa.

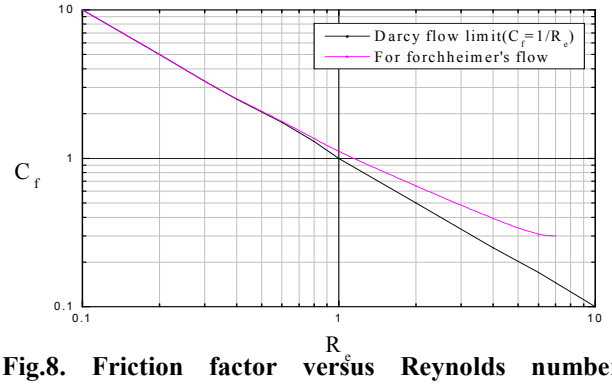

Fig.8. Friction factor versus Reynolds number relation.

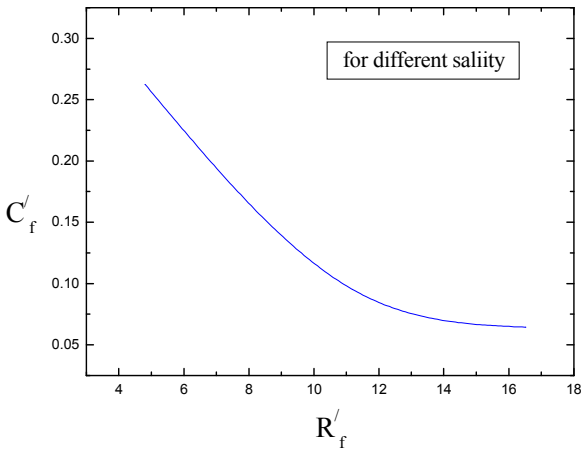

Fig.9. Graphical representation of modified Reynolds number versus modified friction factor.

Table-6. The physico-chemical properties of water samples.

Sl No	pH	Specific Conductivity [micromhos /cm] at 25^0C	Bicarbonate CO_3^- in ppm	Chloride (Cl^-) in ppm	Total Hardness $CaCO_3$ ppm	TDS in ppm
1	8.61	1040	280	70	250	666
2	7.29	16000	570	6900	2480	10240
3	8.14	1190	450	30	280	762
4	7.72	6700	100	2900	1500	4288
5	7.63	3300	210	1120	660	2112
6	7.77	1900	240	580	400	1216
7	8.50	470	250	50	120	301
8	7.80	26000	180	11400	3570	16640
9.	7.38	550	420	60	200	352
10	7.86	1350	240	360	410	864
11	7.36	1380	310	310	490	883
12	7.68	490	490	30	250	314
13	7.76	450	330	20	110	288
14	7.38	1900	340	560	550	1216
15	8.19	580	280	60	210	371
16	7.75	810	330	110	180	518
17	7.84	810	410	90	260	518
18	7.18	850	360	100	230	544
19	7.67	1230	310	280	270	787
20	7.17	560	250	70	150	358
21	7.47	480	270	40	290	307
22	7.55	4700	250	1580	660	3008
23	7.71	910	280	150	100	582
24	7.67	3900	200	1220	560	2496
25	7.71	920	230	100	40	589
26	7.65	970	250	140	50	621
27	8.64	1590	140	450	240	1018
28	7.54	1010	200	160	440	646
29	7.31	3100	100	950	560	1984

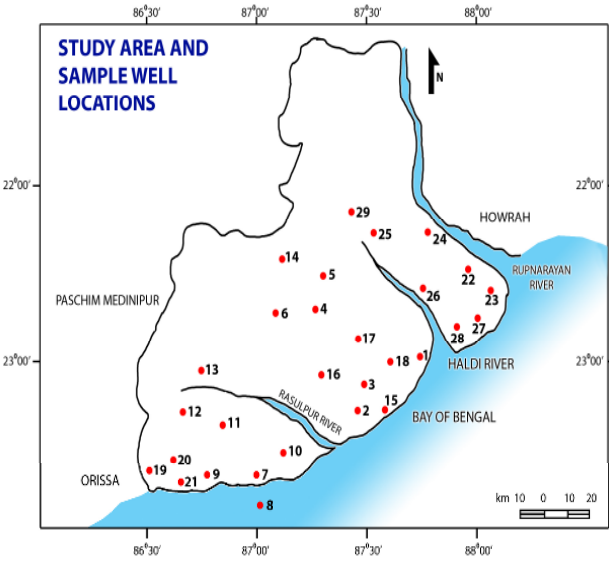

Fig.10. The field study area.

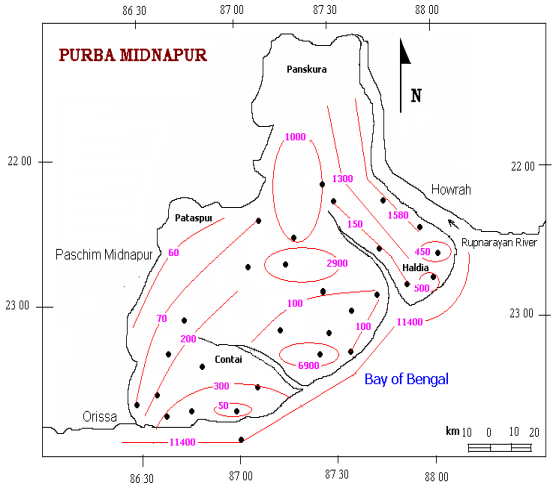

Fig.12. Contours for chloride concentrations.

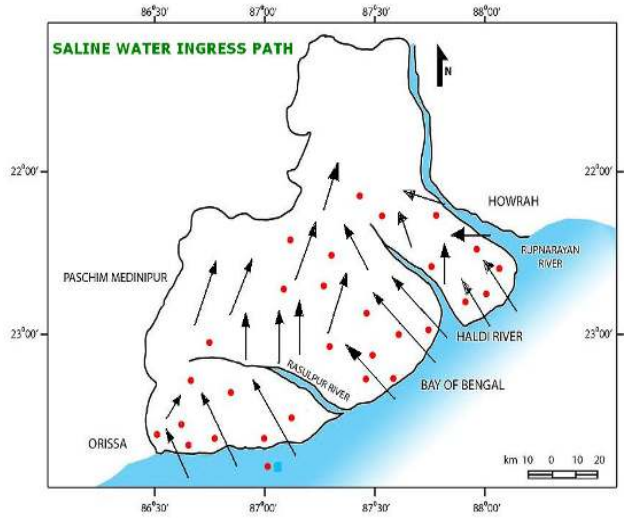

Fig. 11. Probable path of saline water ingress.

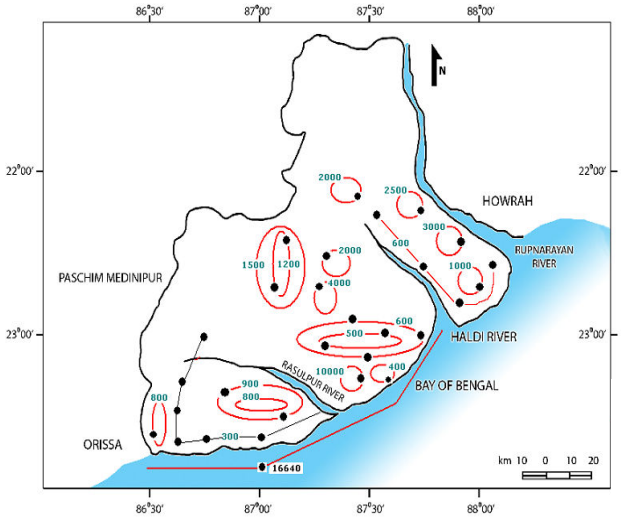

Fig.13. Contours for concentration of Dissolved Solids.

8 Conclusion

From the entire investigation the following conclusion are drawn :

- From the model test on stratified fluid and the representation, one mixing zone has been found and that represents the Turbulence zone. On that zone Reynolds number (R_e) in the range of Forchheimer's flow or in the range of nonlinear flow range.
- The phreatic lines in saline water intrusion and the interfaces in fresh water recharge are observed to be of irregular pattern. In case of saline water intrusion, the phreatic line at any time instance slopes down from the inlet end with a sudden change in slope at a normalized distance of 0.3 to 0.5. With the advent of time, the phreatic line translates gradually further towards the downstream.
- For fresh water recharge, the interface gradually slopes towards the downstream end in advent of time. The time variation of normalized y-coordinates of the interface at different locations, although of irregular pattern, the slopes are observed to be sufficiently small.
- From the results of the Friction factor and Reynolds number for Darcy's and Forchheimer's flow it can be concluded that, if the Reynolds number increases the friction factor decreases. And also for modified Reynolds number versus modified friction factor plot, it can be says that, C_f' and R_e' are changes inversely proportional way. Initially it decreases frequently, but after a limit the rate of decrease in quit slow.
- More importantly, diffusion between fluids of two different densities is observed to take place indicating absence of any sharp interface at mixing zone.
- From the field investigation carried out at a coastal zone of east coast of India, the probable path of saline water ingress has been estimated. The contours for chloride concentration and total dissolved solids in the aquifer groundwater have also been plotted.

References:

[1]Bhattacharya, A. K., Basack, S. and Mohapatra, P., "Non-Linear Flow of Saline Water through Porous Media", *Proceedings, 2nd BSME-ASME International Conference on Thermal Engineering*, 2004, Bangladesh, pp. 340-345.

[2]Cooper, H.H., Jr., "A Hypothesis concerning the Dynamic Balance of Fresh Water and Salt Water in a Coastal Aquifer", *U.S. Geological Survey Water-Supply Paper 1613–C*, 1964, pp. 1–12.

[3]Dagan, G. and Bear, J., "Solving the Problem of Local Interface Upconing in a Coastal Aquifer by the Method of Small Perturbations", *Journal of Hydraulic Research*, Vol.6, No.1,1968, pp.15-44.

[4]Darcy, H, "Les Fontaines Publiques de la ville", *dijion, Dalmont*, 1856, Paris.

[5]Forchheimer, P., Wasserbeweguing durch Boden, Z. Ver. Deutsch Ing., Vol.45, No.1901, pp: 1782-1788.

[6]Taniguchi, M., Burnett, W.C., Cable, J.E. and Turner, J.V., "Investigation of Submarine Ground Water Discharge", *Hydrology Process*, Vol. 16, No.2, 2002, pp. 121-134.